Potential Upstream Regulators of Cannabinoid Receptor 1 Signaling in Prostate Cancer: A Bayesian Network Analysis of Data From a Tissue Microarray

Jenny Häggström,[1] Mariateresa Cipriano,[2] Linus Plym Forshell,[2] Emma Persson,[3] Peter Hammarsten,[4] Nephi Stella,[5] and Christopher J. Fowler[2]*

[1]*Department of Statistics, Umeå School of Business and Economics, Umeå University, Umeå, Sweden*
[2]*Department of Pharmacology and Clinical Neuroscience, Umeå University, Umeå, Sweden*
[3]*Department of Radiation Sciences, Oncology, Umeå University, Umeå, Sweden*
[4]*Department of Medical Biosciences, Pathology, Umeå University, Umeå, Sweden*
[5]*Department of Pharmacology, Psychiatry and Behavioral Sciences, University of Washington, Seattle, Washington*

BACKGROUND. The endocannabinoid system regulates cancer cell proliferation, and in prostate cancer a high cannabinoid CB_1 receptor expression is associated with a poor prognosis. Down-stream mediators of CB_1 receptor signaling in prostate cancer are known, but information on potential upstream regulators is lacking.

RESULTS. Data from a well-characterized tumor tissue microarray were used for a Bayesian network analysis using the max-min hill-climbing method. In non-malignant tissue samples, a directionality of pEGFR (the phosphorylated form of the epidermal growth factor receptor) → CB_1 receptors were found regardless as to whether the endocannabinoid metabolizing enzyme fatty acid amide hydrolase (FAAH) was included as a parameter. A similar result was found in the tumor tissue, but only when FAAH was included in the analysis. A second regulatory pathway, from the growth factor receptor ErbB2 → FAAH was also identified in the tumor samples. Transfection of AT1 prostate cancer cells with CB_1 receptors induced a sensitivity to the growth-inhibiting effects of the CB receptor agonist CP55,940. The sensitivity was not dependent upon the level of receptor expression. Thus a high CB_1 receptor expression alone does not drive the cells towards a survival phenotype in the presence of a CB receptor agonist.

CONCLUSIONS. The data identify two potential regulators of the endocannabinoid system in prostate cancer and allow the construction of a model of a dysregulated endocannabinoid signaling network in this tumor. Further studies should be designed to test the veracity of the predictions of the network analysis in prostate cancer and other solid tumors. *Prostate 74: 1107–1117, 2014.* © 2014 The Authors. *The Prostate* published by Wiley Periodicals, Inc. This is an open access article under the terms of the Creative Commons Attribution-NonCommercial-NoDerivs License, which permits use and distribution in any medium, provided the original work is properly cited, the use is non-commercial and no modifications or adaptations are made.

KEY WORDS: prostate cancer; epidermal growth factor; cannabinoid receptor; fatty acid amide hydrolase; directed acyclic graph

INTRODUCTION

In 1975, Munson and colleagues reported that $\triangle^9$-tetrahydrocannabinol, the main psychoactive constituent of cannabis, reduced tumor growth, and increased life span in a xenograft model of lung cancer [1]. Since then, a large number of studies have demonstrated that the endocannabinoid system, defined here as cannabinoid CB_1 and CB_2 receptors, their endogenous ligands anandamide (AEA) and 2-arachidonoylglycerol (2-AG), and their synthetic and metabolic enzymes, control cancer cell proliferation, and migration [2–5]. The prostate gland expresses a functional epithelial CB_1 receptor, which in the rat is involved in the control of the contraction of the gland [6,7], and its expression is increased in prostate cancer (Pca) cells [8,9], as is the expression of several endocannabinoid metabolizing enzymes, such as fatty acid amide hydrolase (FAAH) [10,11], cyclooxygenase-2 [12], and acylglycerol kinase [13]. Data from cell cultures and animal models are consistent with the hypothesis that the circulating endocannabinoid system can dampen the proliferation and invasivity of Pca cells [14–17], although mitogenic effects of low concentrations of CB_1 receptor agonists secondary to activation of the Akt signaling pathway have been described [18]. In Pca tumor samples, CB_1 receptor scores and pAkt scores are correlated and show a significant interaction term in ordinal regression analyses with the Gleason score as the dependent variable [19].

Whilst down-stream mediators of CB_1 receptor signaling in Pca have been well-investigated (review, see [4]), little is known concerning potential upstream regulators of this receptor. One way of identifying potential candidates is to undertake a Bayesian network analysis of available tissue microarray data, to create a directed acyclic graph. This method uses probabilistic theory to create a map of the nodes (the variables chosen) and edges (shown as arrows) with directionality, and where cyclicity is not allowed (for review, see [20]). It has been used successfully in a number of very different biological situations ranging from mapping the evolution of Thoracian barnacles to delineating signaling networks in human primary naïve CD4$^+$ T cells [21,22]. In the present study, we have utilized this approach and identified the activated (phosphorylated) form of the epidermal growth factor receptor (pEGFR) as a potential upstream regulator of CB_1 receptors in Pca.

MATERIALS AND METHODS

Patient Material and Immunochemistry

The tissue material (formalin-fixed, paraffin-embedded samples) was collected at the Regional Hospital,

Västerås, Sweden, between 1975 and 1991 from a total of 419 patients consecutively diagnosed with Pca following transurethral resection for lower urinary tract symptoms [23,24]. The patients had not received anti-cancer therapy before undergoing the transurethral resection procedure. The distribution of Gleason scores (number [%] of cases) in the material was 4–5, 98 (23%); 6, 110 (26%); 7, 72 (17%); 8–10, 139 (33%). The tumor stage (when given in the database) was 1a–1b, 210 (51%); 2, 107 (26%); 3, 81 (20%); 4, 13 (3%). A total of 48 (15%) of 322 cases were found to have metastases (bone scan) at diagnosis. The patients were followed until 2003 (for further details, see [23] [for the first 305 cases] and [24] [for the entire dataset]). Tissue microarrays were constructed and in general between 1 and 8 cores (usually 5, including both primary and secondary Gleason grade areas; tumor tissue) could be scored for the parameter in question. The mean % of the specimen that was tumor associated (% ca) varied from 5% to 100%, with cases >5% showing a poorer prognosis than those ≤5% [23]. The number (%) of cases at % ca levels of 5, 10–25, 30–50, 55–75, and 80–100, were 81 (19%), 125 (30%), 56 (13%), 46 (11%), and 111 (26%), respectively. Immunoreactive scores for the epithelial CB_1 receptor (CB_1R), EGFR, pEGFR, ErbB2, LRIG1, platelet-derived growth factor receptor ß (PDFRß), androgen receptor (AR), von Willebrand factor (vWf), endoglin, hyaluronan, mast cell, and FAAH used in the present study were taken from our database (see [11,19,25–32] for published data and details of the methodologies). For the main parameters used here with the exception of LRIG1, the cores were scored on the basis of intensity and distribution to give a composite value. Thus, for example, a core scored at 25% intensity 1, 25% intensity 2, and 50% intensity 3 for the biomarker in question would score $0.25 \times 1 + 0.25 \times 2 + 0.5 \times 3 = 2.25$. The intensity ranges for CB_1R and ErbB2 were 0–4, pEGFR 0–5, LRIG1 0–2, and FAAH 0–3. The composite score thus represents a measure of the "loading" of the tumor for the parameter in question. For some parameters (e.g., FAAH [11]), the scores were made upon microscopic evaluation of the cores. This was also the case for the CB_1 receptors in our initial study using an intensity range of 0–3 [33]. However, we rescored digital images of the samples using a range 0–4 and two investigators, who returned scores with a very high inter-rater reliability (Chronbach's alpha of 0.94 for an intra-class correlation analysis using a mixed model and testing for consistency [19]) and we used these values here. In both these examples, the investigators were blind to the clinical data, other than the obvious morphological characteristics of the samples, when scoring the cores. The antibodies used for the main parameters were: CB_1R, AbCam cat. no. 23703, lot no. 280229; pEGFR, Cell Signaling TYR845

lot 4; FAAH, an antibody raised against the last 102 amino acids of rat FAAH and kindly provided by Prof. Ken Mackie, Indiana University, USA; LRIG1, Agrisera rabbit polyclonal LRIG1-151; ErbB2, mouse c-erbB-2 Prediluted Cocktail Antibody, Biocare ([11,27,30,33] and unpublished data). The Ventana system was used for high-throughput immunostaining of the samples (see the above papers for details).

The research ethical committee at Umeå university hospital (Regional Ethical Review Board in Umeå, Sweden) approved of the study and waived the need for informed consent. In the database used for the analyses, the tissue samples were given a case number and year, and the patient names were not indicated in the database.

CB_1 Receptor-Transfected AT1 Cells

R3327-AT1 rat Dunning prostate cancer cells (ATCC, Manassas, VA; hereafter called AT1 cells) were cultured in RPMI medium (10% FBS, 1% penicillin-streptomycin, 2 mM glutamine, 250 nM dexamethasone). The cells were seeded out at 250,000–300,000 cells *per* well in 6-well plates. The next day, the cells were transfected either with the control plasmid (pIRES2-eGFP) or the murine CB_1 receptor-containing plasmid (pIRES2-mCB1-eGFP) using the TransIT®-prostate transfection kit and protocol supplied by the Mirus Corporation (Madison, WI). For details of the plasmids, see [34]. Initial experiments indicated that the ratio of DNA: TransIT®-reagent: Prostate Boost reagent (supplied in the kit) of 3 μg: 10 μl: 10 μl gave the best transfections. After incubation with the prostate boost reagent for 20 min, chloroquine (25 μM final concentration) was added and the samples were incubated for 150 min. Thereafter, the transfection media was replaced by media containing 10% (v/v) glycerol, the cells were incubated for 3 min at room temperature followed by two washes with warm phosphate-buffered saline. Finally, the culture media was added and the cells were allowed to grow for 48–72 hr prior to assessing the number of eGFP-positive cells by FACS analysis. Cells were selected in growth medium containing G418 (400 μg/ml). This protocol provided cells with a very large range of fluorescence intensity on FACS. Initial experiments indicated that incubation with a low concentration of CP55,940 ((−)-cis-3-[2-hydroxy-4-(1,1-dimethylheptyl)phenyl]-trans-4-(3-hydroxypropyl)cyclohexanol; Tocris Cookson, Bristol, UK), resulted in a loss of the highest intensity cells for both the eGFP- and CB_1/eGFP-transfected cells, suggesting that at this level of transfection, the plasmid load is detrimental to cell survival regardless of the absence or presence of the murine CB_1 receptors. In consequence, these cells were removed by a 6-day incubation of both eGFP- and CB_1/eGFP-transfected cells with 10 nM CP55,940 after which the cells were cultured for 2 weeks to amplify the stocks. In the experiments reported here, the cells, in six-well culture plates, were then incubated with test compounds for 3 days, and cell proliferation and fluorescence intensities were determined by FACS using a Guava easy-Cyte™ Flow Cytometer (Merck Millipore).

Statistics

Three statistical software programmes were used. Two-way ANOVA and Spearman's correlation coefficients were determined using the statistical package built into the GraphPad Prism 5 and 6 computer programmes for the Macintosh (GraphPad Software Inc., San Diego, CA). Univariate regressions using the general linear model were undertaken using SPSS software (IBM SPSS statistics version 22 for the Macintosh, IBM Corporation, Armonk, NY). The directed acyclic graphs and bootstrap analyses were calculated using the function mmhc in the bnlearn package of the R computer programme [35].

RESULTS

Interconnection between CB_1R, pEGFR, ErbB2, LRIG1, and FAAH in prostate tumor tissue.

To identify potential components of a network that encompasses CB_1 receptors and is involved in Pca cell tumourigenesis, we undertook a simple bivariate correlation analysis with a number of different biochemical markers that have been scored in a well-characterized Pca tumor microarray (see [11,19,23–33] for hitherto published data). Using a cut-off Spearman's rho value of 0.2, four parameters were identified: pEGFR, FAAH (as reported previously, [11,32]), the growth factor receptor ErbB2, and the EGFR regulatory protein LRIG1 (leucine-rich and immunoglobulin-like domains protein 1) (Fig. 1). These associations were not seen in the non-malignant tissue (Fig. 1).

Although the sample set were consecutive cases, the nature of their accruement (diagnosis following transurethral resection) means that they are not an unselected set of *all* Pca cases, since cases with Pca but not in the resected region will have been missed. Further, there has been a shift over time in the severity of the disease (i.e., relative incidence of the different tumor stages and Gleason scores) at diagnosis since the introduction of PSA testing [36]. In order to gain information as to whether this could be a limiting factor in our study, we conducted univariate regressions using the general linear model with the tumor CB_1 receptor scores as the dependent variables, the
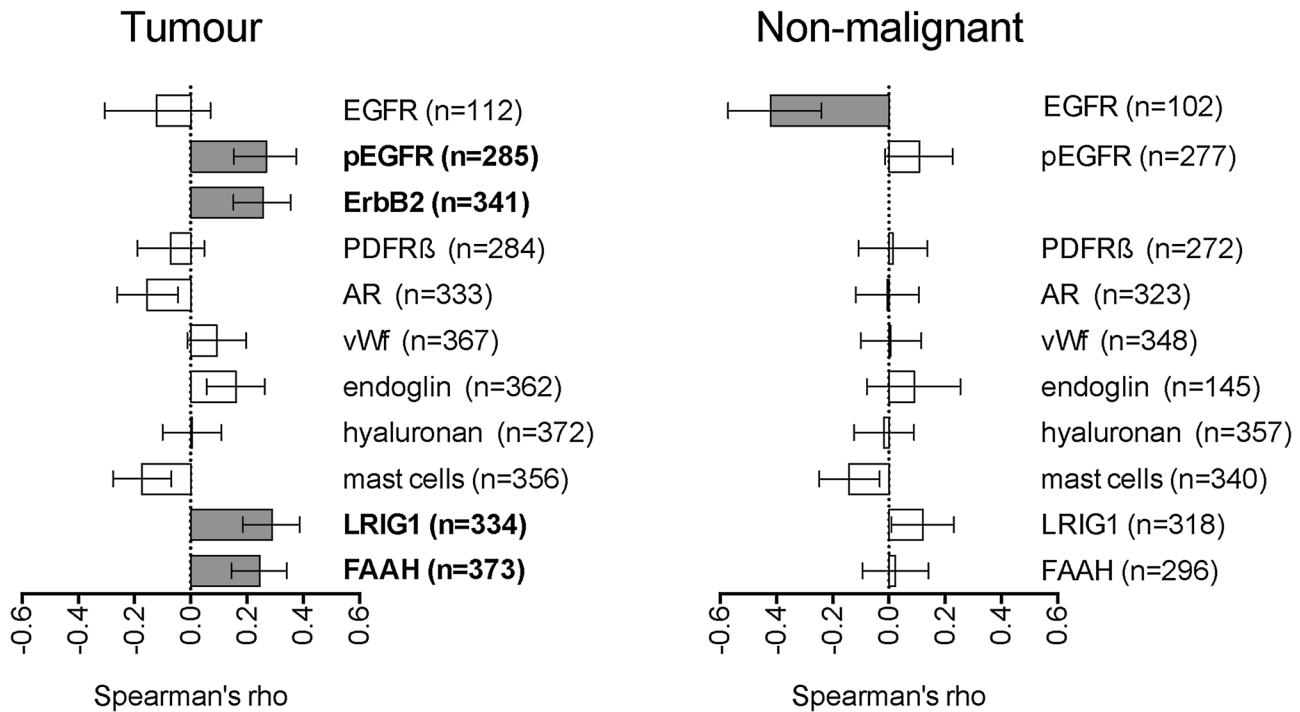
Tumour

Non-malignant

Fig. 1. Bivariate correlations between CB$_1$ receptor scores and other parameters in the database. Shown are the Spearman rho values and the 95% confidence limits. Values where the Spearman rho value was >0.2 are shaded gray. Note that for the non-malignant scores, FAAH and pEGFR are available for both basal and luminal epithelial cells. The luminal scores were used here. Note also that the sample size for non-phosphorylated EGFR is much smaller than for pEGFR and most of the other parameters, thereby precluding its use in the subsequent Bayesian network analyses.

Gleason scores (grouped as 4–6, 7, and 8–10) and the tumor stages (grouped as 1a–1b, 2, 3, and 4) as fixed factors, and each of the four parameters identified above as co-variates. In each case, the co-variates contributed significantly to the regression. The unstandardized beta weights (with 95% confidence intervals in brackets) for the four co-variates were: pEGFR, 0.125 (0.039–0.210), $P < 0.005$; FAAH, 0.224 (0.091–0.356), $P < 0.001$; ErbB2, 0.212 (0.117–0.306), $P < 0.0001$; LRIG1, 0.345 (0.161–0.530), $P < 0.0005$. In all cases, the Levene's test of equality of error variances was satisfied ($P > 0.3$). This indicates that the associations between the four parameters and the CB$_1$ receptor score in the tumor tissue remain even when controlled for the severity of the disease at diagnosis.

For the non-malignant samples, the data available in the database was used to construct two directed acyclic graphs, one with three variables (CB$_1$R, luminal epithelial pEGFR and LRIG1), and one with four variables (CB$_1$R, luminal epithelial pEGFR, LRIG1, and luminal epithelial FAAH; non-malignant ErbB2 was not scored in a sufficient number of cores to be used). The method used to conduct the analysis was the max-min hill-climbing algorithm, which gives every possible network a score, and outlines a network with the highest score that best fits the data [37].

Further, the datasets were subjected to a bootstrap analysis and the process was repeated 1,000 times to estimate the uncertainty in the analyses. A bootstrap dataset of the same size as the original dataset is obtained by random sampling with replacement from the observations in the original data. For each bootstrap sample, a directed acyclic graph was constructed, and then the frequency of the possible combinations was obtained. This information was then incorporated in the directed acyclic graphs for the original complete dataset where the thickness of the edges indicates the reliability of the measure. The method requires that, for a given sample, there are no missing values. Thus, for example, if a network comprising three parameters is constructed, then every case must have scores for the parameters in question. This means that the optimal network size will be a trade-off between the number of parameters comprising the network and the number of cases scored for all the parameters. Sample sizes used here are given in the figure legends.

For the three-variable analysis, an edge pEGFR → CB$_1$R was found for the non-malignant tissue samples, the directionality of the line being much greater than for CB$_1$R → pEGFR in the bootstrap analyses (Fig. 2A). An edge LRIG1 → pEGFR was also found for the
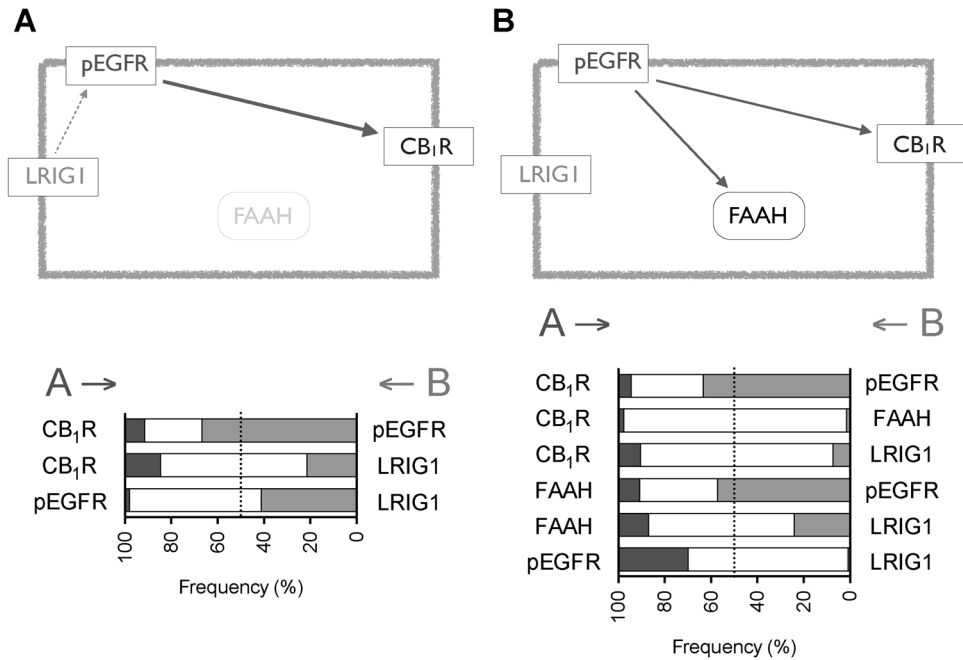
Fig. 2. Bayesian network inference analyses of CB$_1$R, pEGFR, LRIGI, and FAAH immunoreactive scores for prostate non-malignant tissue samples obtained at diagnosis. The function mmhc in the bnlearn package of the R computer programme was used. The panels show the directed acyclic graphs for the complete datasets for the fully visible variables shown in the figure: (**A**) CB$_1$R, luminal epithelial pEGFR and LRIGI (n = 263) (**B**) CB$_1$R, luminal epithelial pEGFR, LRIGI and luminal epithelial FAAH (n = 221). Bootstrap analyses of the Bayesian network inference analyses are shown underneath the directed acyclic graphs. The graphs show the percentage of times, out of 1,000 trials, that the direction A → B (dark grey), B → A (light grey), or no preference (white) was found. The dotted line is set at 50% to aid the reader. This information was then incorporated into the graphs for the complete datasets, whereby the thicknesses of the arrows indicate the confidence of the edges (i.e., how often it was found in the bootstrap analyses), divided into two groups: >65% (pEGFR → CB$_1$R in panel **A**) and >50% (pEGFR → CB$_1$R and pEGFR → FAAH in panel **B**). The dotted arrow in Panel **A** shows where the edge for the whole dataset was not supported by the bootstrap analyses.

complete dataset, but this was deemed to be unreliable in the bootstrap analysis, since its frequency was lower than that for no preference. The addition of FAAH to the dataset did not change the observed pattern pEGFR → CB$_1$R >> CB$_1$R → pEGFR and suggested an additional edge pEGFR → FAAH (Fig. 2B).

For the tumor samples, the networks obtained for a three-variable analysis (CB$_1$R, pEGFR, and ErbB2, i.e., the three receptors in the sample), two four-variable analyses (the receptors and LRIG1; the receptors and FAAH), and a five-variable analysis (the receptors, LRIG1 and FAAH) are shown in Figure 3 for the whole patient sample ("original data") and the bootstrap analyses shown in Figure 4. In this case, the observed direction of the edges was highly dependent upon the inclusion, or not, of FAAH. When FAAH was excluded from the analyses, the directionality of the edges was from CB$_1$R to the growth factor receptors and not vice versa (Fig. 3A, B), whereas when FAAH was included as a parameter, the directionality of the association between pEGFR and CB$_1$R was reversed, that is, to be the same as seen in the non-malignant tissue (Fig. 3C, D).

Two other edges, LRIG1 → ErbB2 and ErbB2 → FAAH were seen in the tumor samples (Fig. 3B–D). There is some dispute as to the level of expression of ErbB2 in Pca, not the least due to the use of different antibodies [38]. In consequence, we reanalyzed the tumor data excluding this parameter, and found that for both CB$_1$R, pEGFR and LRIG1 as variables (n = 271), and for CB$_1$R, pEGFR, LRIG1, and FAAH as variables (n = 268), the directed acyclical graphs gave the edge pEGFR → CB$_1$R with a frequency of 65% and 62%, respectively, in the bootstrap analyses (data not shown).

A high CB$_1$ receptor expression per se is insufficient to confer a selective survival of Pca cells to CB$_1$ receptor stimulation.

The network analysis identifies CB$_1$ receptors as down-stream of the EGFR, but does not provide any information as to whether a high CB$_1$ receptor expression directly biases tumor cells towards survival in the presence of a CB receptor agonist, such as has been seen in astrocytoma clones transfected with this receptor [34]. In order to shed light on this possibility, AT1
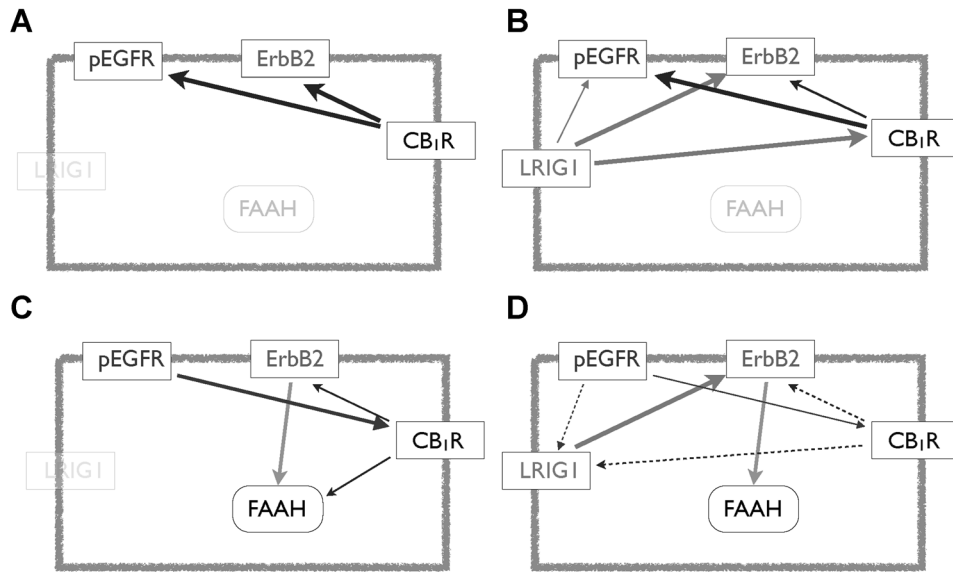
Fig. 3. Bayesian network inference analyses of CB₁R, pEGFR, ErbB2, LRIGI, and FAAH immunoreactive scores for prostate tumour samples obtained at diagnosis. The function mmhc in the bnlearn package of the R computer programme was used. The panels show the directed acyclic graphs for the original datasets for the fully visible variables shown in the figure: (**A**) CB₁R, pEGFR, and ErbB2 (n = 274); (**B**) LRIGI, CB₁R, pEGFR, and ErbB2 (n = 270); (**C**) FAAH, CB₁R, pEGFR, and ErbB2 (n = 271); and (**D**) FAAH, LRIGI, CB₁R, pEGFR, and ErbB2 (n = 267). The thicknesses of the arrows indicate the confidence of the edges (i.e., how often it was found in the bootstrap analyses shown in Fig. 4), divided into four groups: >85% (e.g., CB₁R → pEGFR in panel **A**); >65% (e.g., pEGFR → CB₁R in panel **C**); >50% (e.g., CB₁R → ErbB2 in panel **B**); and <50% but more frequent than B → A or for no preference (e.g., pEGFR → CB₁R in panel **D**). The dotted arrows show where the edges for the whole dataset were not supported by the bootstrap analyses.

prostate cancer cells were transfected with either eGFP or CB₁/eGFP plasmids (the same plasmids used in [34]). This cell line is one of the R3327 Dunning rat prostatic tumor sublines, which show different metastatic abilities when injected into syngenic Copenhagen rats [39]. It has been used in vivo in orthotopic studies to characterize tumor growth in the ventral prostate after different interventions [40,41], and is thus a rather useful rodent cell line. We have previously characterized it with respect to its ability to accumulate and metabolize endocannabinoids [42,43], but to our knowledge the effect of CB₁ receptor activation upon AT-1 cell survival has not been studied.

Successful transfection with the receptor was confirmed by RT-PCR, where the level of mRNA signal for the CB₁ receptor was in the ratio 1: 2.6: 750 for untransfected, eGFP- and CB₁/eGFP-transfected cell populations (data not shown). Rather than select individual clones with different receptor expression levels, we elected to utilize the variation in transfection efficiency of the unselected cells to mimic the large variation in CB₁ receptor expression seen in the Pca tumor arrays [19]. In the cells transfected with the reporter protein eGFP alone, the CB receptor agonist CP55,940 produced a weak mitogenic effect, whereas in the cells transfected with the plasmid encoding CB₁ receptors and eGFP, nanomolar concentrations of

CP55,940 reduced the cell density (Fig. 5). Thus, introduction of the CB₁ receptor into the cells conferred a changed sensitivity to CP55,940. Notably, the sensitivity to this agonist was the same for cells with expression levels above the median for the cell population as for those with expression levels below the median (Fig. 5). This result suggests that in the model system used, cells expressing levels of CB₁ receptor that are above the median value do not exhibit an advantage in terms of cell proliferation and resistance to the anti-proliferative effects of CP55,940.

DISCUSSION

In the present study, Bayesian network analyses were undertaken on Pca tissue microarray data to identify potential upstream regulators of CB₁ receptors. The strength of the study lies in the nature of the samples used, in that they were taken prior to diagnosis, and thus the parameters under study are not influenced by anti-cancer treatment of the patients. Further, the Bayesian methodology has proven useful in identifying potential biological networks [21,22]. This notwithstanding, at the outset, several potential limitations to the approach used in the present study should be considered. First, the model used assumes the data are continuous, whereas in fact they are
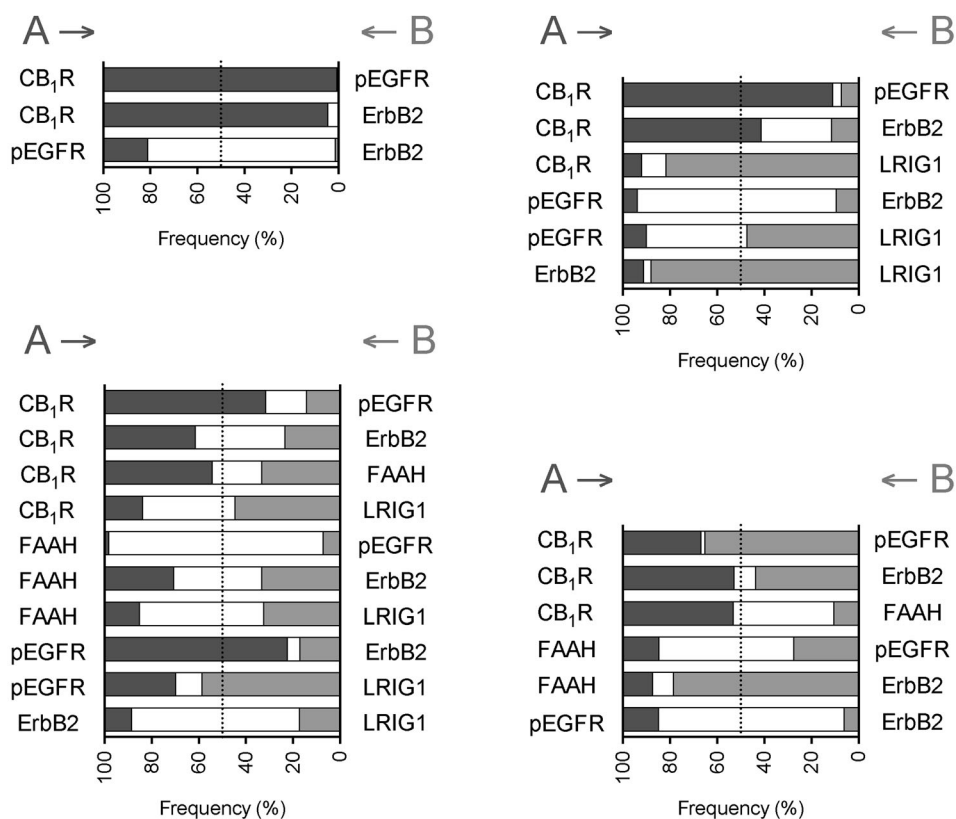
Fig. 4. Bootstrap analyses of the Bayesian network inference analyses shown in Figure 3. The graphs show the percentage of times, out of 1,000 trials, that the directions A → B (dark grey), B → A (light grey), or no preference (white) was found. The graphs are: **top left**, CB_1R, pEGFR, and ErbB2; **top right**, LRIGI, CB_1R, pEGFR, and ErbB2; **bottom right**, FAAH, CB_1R, pEGFR, and ErbB2; **bottom left**, FAAH, LRIGI, CB_1R, pEGFR, and ErbB2. The dotted line is set at 50% to aid the reader.
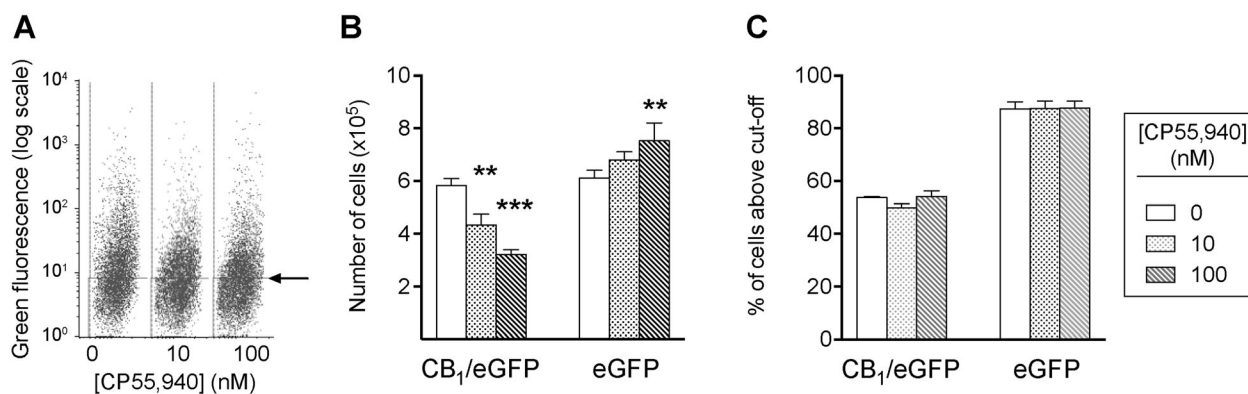

Fig. 5. Effect of the CB receptor agonist CP55,940 upon the density of ATI cells transfected with CB_1 receptors. Panel **A** shows a representative FACS for ATI cells transfected with the CB_1/eGFP plasmid and treated for 3 days with 0, 10, or 100 nM CP55,940. Panel **B** shows the number of cells and Panel **C** the % of cells above the cut-off chosen (shown as a dashed horizontal line marked with the arrow in Panel **A**) following CP55,940 treatment. Panels **B** and **C** show means and s.e.m. values, n = 6. The number n refers to the number of series run for FACS from each six well plate; in some experiments two series were run on the same day. In Panel **A**, a two-way ANOVA for repeated measures (matching for CP55,940) gave a significant interaction ($F_{2,20} = 24.86$, $P < 0.0001$). **$P < 0.01$, ***$P < 0.001$, Sidak's multiple comparison test versus the corresponding value in the absence of CP55,940. In Panel **C**, there was no significant interaction ($F_{2,20} = 1.56$, $P = 0.23$) or main effect of CP55,940 ($P_{2,20} = 1.50$, $P = 0.25$) although there was a significant effect of the transfection with respect to the proportion of cells above the cut-off for the eGFP-transfected cells than for the CB_1/eGFP-transfected cells ($P_{1,10} = 159$, $P < 0.0001$).

ordinal. However, given that the score is a composite measure of intensity $\times$ distribution, that is, the relative load in the tissue, it takes on a large number of different values. For tumor CB_1R, for example, the cases scored for this parameter are distributed among 52 different scores between 0.25 and 4. Treating such a variable as continuous in the analysis is not unusual. Second, the data are from a single cohort, and although we have used bootstrapping as a measure of the robustness of the data, it would be well worth replicating the study in a second cohort. Third, the network only considers the available data and does not consider other potential regulatory elements. One such element known to be involved in the pathogenesis of Pca is interleukin-4 [44], which influences both CB_1 receptor and FAAH expression in cells [11,45,46]. However, as pointed out in the results, inclusion of additional parameters, when available, will reduce the number of cases scored for all parameters. Fourth, the directed acyclic graphs do not allow bidirectional signaling. This is relevant, given the finding in cultured Pca cells that cannabinoids reduce the proliferative response to EGF by down-regulating EGFR [15] (in contrast to the situation in cell lines from some other cancer forms (squamous cell carcinoma, bladder carcinoma, astrocytoma and kidney cancer) where cannabinoids increase both EGFR phosphorylation and cell proliferation [47]). Finally, the data are only as good as the antibodies used. There has been, for example, debate as to the usefulness of some of the CB_1 receptor antibodies available [48]. However, we established that the CB_1R antibody used in the tissue microarray showed the appropriate pattern of immunoreactivity in the brain, and that staining was absent in both the brain and prostate of CB_1R knockout mice [33]. Thus, although the methodology is not without issues and the results should be considered in this light, they do form the basis for hypothesis testing in relevant biological systems.

In non-malignant tissue, the analyses indicated that the CB_1 receptor expression was down-stream of pEGFR, rather than vice versa, and that this pattern was seen regardless of whether FAAH was included in the analyses. In the malignant tissue, the same relationship between pEGFR and CB_1 receptor expression was seen, but only when FAAH was included. The difference in "FAAH-dependency" between the non-malignant and tumor sample is in addition to be expected, given the greater expression level of FAAH in the tumor samples than in the non-malignant luminal tissue [11]. A second novel observation was the edge ErbB2 $\rightarrow$ FAAH in the tumor samples. To our knowledge, EGFR- and ErbB2-receptor mediated regulation of CB_1 receptor and FAAH expression, respectively, have not been reported for prostate tissue, and

thus the current study identifies potential novel regulatory pathways. With respect to the former, we have preliminary data suggesting that long-term treatment with EGF indeed increased the mRNA for CB_1 receptors in Pca cells in culture in a manner dependent upon the basal CB_1 receptor expression, which was not stable in the cells (M. Cipriano and C. J. Fowler, unpublished data), but more systematic data is needed. The ability of ErbB2 to regulate FAAH has not been studied, although conceptually it is highly possible, given that in rat hippocampal slices, treatment with the ErbB receptor tyrosine kinase ligand neuroregulin-1 for 8–11 days increases the expression of monoacylglycerol lipase, the main hydrolytic enzyme for the endocannabinoid 2-AG [49].

In addition to identifying potential upstream modulators of endocannabinoid signaling, the network analysis can provide conceptual data for formulation of novel hypotheses. In the present context, it allows us to suggest a way in which the CB_1 receptor is involved in the pathogenesis of Pca. Our working model is based on the network analysis, the study of CB_1 agonist effects upon EGF-stimulated Pca cells [15], the observations of down-stream activation of Akt [18,19], and the transfected AT1 cell data presented here which suggest that a high CB_1 receptor expression alone is not sufficient to drive the cells towards a survival phenotype in the presence of a CB receptor agonist. The model is summarized in Figure 6. In non-malignant tissue, normal EGF signaling produces both an array of cellular responses [51] and increases CB_1 receptor expression. These then respond to the circulating levels of endocannabinoids and decrease EGFR expression [15], thus operating as a negative feedback regulatory mechanism. The findings that the 2-AG metabolizing enzyme acylglycerol kinase is expressed in Pca tumors to a higher level than in matched non-malignant tissue, and its down-regulation inhibits the motility of Pca cells in response to EGF [13] also support this model. In the tumor tissue, EGF-mediated signaling is overactive [27,52] and FAAH, acylglycerol kinase and other enzymes known to metabolize endocannabinoids (such as cyclooxygenase-2) are up-regulated [10–13], in the case of FAAH perhaps due in part to aberrant ErbB2 signaling that has been reported in some Pca cases [38,53]. This would result in a reduction in the levels of circulating endocannabinoids, thus weakening the feedback regulatory pathway.

It should be stressed that the model as shown in Figure 6 is theoretical rather that proven, although supported by current data. Clearly, it is important to determine in experimental models, cell cultures and tumor samples whether the model is valid. Additionally, given that a high tumor CB_1 receptor expression is
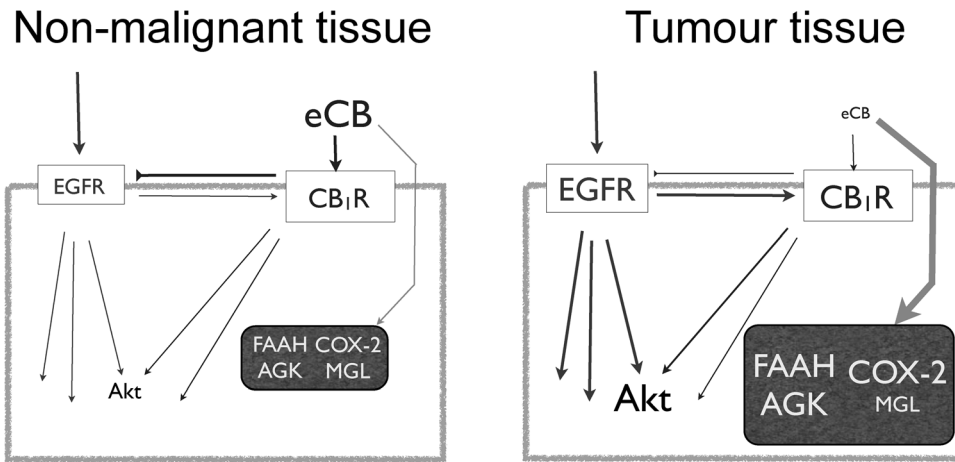
Fig. 6. Model of the EGFR—CB$_1$ receptor signaling network in Pca. The size of the typeface and the thickness of the lines is an indication of the activity in the pathways. Note that for the intracellular pathways for CB$_1$ receptors, both pro- and anti-apoptotic pathways have been reported [4]. Abbreviations: AGK, acylglycerol kinase; COX-2, cyclooxygenase-2; eCB, endocannabinoid; MGL, monoacylglycerol lipase. Note that for simplicity the CB$_1$ receptor has been placed on the plasma membrane, whereas in fact it is also found to be active intracellularly [50].

also associated with a poor prognosis in pancreatic cancer and stage II microsatellite-stable colorectal cancer [54,55] (but not hepatocellular carcinomas, [56]), and with the severity of ovarian cancer [57], our study raises the question as to whether similar networks are operative in these systems.

REFERENCES

1. Munson A, Harris L, Friedman M, Dewey W, Carchman R. Antineoplastic activity of cannabinoids. J Nat Cancer Inst 1975; 55:597–602.

2. Freimuth N, Ramer R, Hinz B. Antitumorigenic effects of cannabinoids beyond apoptosis. J Pharmacol Exp Ther 2010;332: 336–344.

3. Díaz-Laviada I. The endocannabinoid system in prostate cancer. Nat Rev Urol 2011;8:553–561.

4. Guindon J, Hohmann AG. The endocannabinoid system and cancer: Therapeutic implication. Br J Pharmacol 2011;163:1447–1463.

5. Velasco G, Sanchez C, Guzmán M. Towards the use of cannabinoids as antitumour agents. Nat Rev Cancer 2012;12:436–444.

6. Ruiz-Llorente L, Sánchez M, Carmena M, Prieto J, Sánchez-Chapado M, Izquierdo A, Díaz-Laviada I. Expression of functionally active cannabinoid receptor CB$_1$ in the human prostate gland. Prostate 2003;54:95–102.

7. Tokanovic S, Malone D, Ventura S. Stimulation of epithelial CB$_1$ receptors inhibits contractions of the rat prostate gland. Br J Pharmacol 2007;150:227–234.

8. Sarfaraz S, Afaq F, Adhami V, Mukhtar H. Cannabinoid receptor as a novel target for the treatment of prostate cancer. Cancer Res 2005;65:1635–1641.

9. Czifra G, Varga A, Nyeste K, Marincsák R, Tóth B, Kovács I, Kovács L, Bíró T. Increased expressions of cannabinoid receptor-1 and transient receptor potential vanilloid-1 in human prostate carcinoma. J Cancer Res Clin Oncol 2009;135:507–514.

10. Endsley M, Thill R, Choudhry I, Williams C, Kajdacsy-Balla A, Campbell W, Nithipatikom K. Expression and function of fatty acid amide hydrolase in prostate cancer. Int J Cancer 2008;123: 1318–1326.

11. Thors L, Bergh A, Persson E, Hammarsten P, Stattin P, Egevad L, Granfors T, Fowler CJ. Fatty acid amide hydrolase in prostate cancer: Association with disease severity and outcome, CB$_1$ receptor expression and regulation by IL-4. PLoS ONE 2010;5: e12275.

12. Shao N, Feng N, Wang Y, Mi Y, Li T, Hua L. Systematic review and meta-analysis of COX-2 expression and polymorphisms in prostate cancer. Mol Biol Rep 2012;39:10997–11004.

13. Bektas M, Payne S, Liu H, Goparaju S, Milstien S, Spiegel S. A novel acylglycerol kinase that produces lysophosphatidic acid modulates cross talk with EGFR in prostate cancer cells. J Cell Biol 2005;169:801–811.

14. Melck D, De Petrocellis L, Orlando P, Bisogno T, Laezza C, Bifulco M, Di Marzo V. Suppression of nerve growth factor trk receptors and prolactin receptors by endocannabinoids leads to inhibition of human breast and prostate cancer cell proliferation. Endocrinology 2000;141:118–126.

15. Mimeault M, Pommery N, Wattez N, Bailly C, Hénichart J-P. Anti-proliferative and apoptotic effects of anandamide in human prostatic cancer cell lines: Implication of epidermal growth factor receptor down-regulation and ceramide production. Prostate 2003;56:1–12.

16. Nithipatikom K, Endsley M, Isbell M, Falck J, Iwamoto Y, Hillard C, Campbell W. 2-Arachidonoylglycerol: A novel inhibitor of androgen-independent prostate cancer cell invasion. Cancer Res 2004;64:8826–8830.

17. Nomura DK, Lombardi DP, Chang JW, Niessen S, Ward AM, Long JZ, Hoover HH, Cravatt BF. Monoacylglycerol lipase exerts dual control over endocannabinoid and fatty acid pathways to support prostate cancer. Chem Biol 2011;18:846–856.

18. Sánchez M, Ruiz-Llorente L, Sánchez A, Díaz-Laviada I. Activation of phosphoinositide 3-kinase/PKB pathway by CB_1 and CB_2 receptors expressed in prostate PC-3 cells. Involvement in Raf-1 stimulation and NGF induction. Cell Signal 2003;15:851–859.

19. Cipriano M, Häggström J, Hammarsten P, Fowler CJ. Association between cannabinoid CB_1 receptor expression and Akt signalling in prostate cancer. PLoS ONE 2013;8:e65798.

20. Markowetz F, Spang R. Inferring cellular networks—A review. BMC Bioinformatics 2007;8(Suppl 6):S5.

21. Pérez-Losada M, Høeg JT, Crandall KA. Unraveling the evolutionary radiation of the thoracican barnacles using molecular and morphological evidence: A comparison of several divergence time estimation approaches. Syst Biol 2004;53:244–264.

22. Sachs K, Perez O, Pe'er D, Lauffenburger DA, Nolan GP. Causal protein-signaling networks derived from multiparameter single-cell data. Science 2005;308:523–529.

23. Egevad L, Granfors T, Karlberg L, Bergh A, Stattin P. Prognostic value of the Gleason score in prostate cancer. BJU Int 2002;89:538–542.

24. Josefsson A, Wikström P, Granfors T, Egevad L, Karlberg L, Stattin P, Bergh A. Tumor size, vascular density and proliferation as prognostic markers in GS6 and GS7 prostate tumors in patients with long follow-up and non-curative treatment. Eur Urol 2005;48:577–583.

25. Wikström P, Marusic J, Stattin P, Bergh A. Low stroma androgen receptor level in normal and tumor prostate tissue is related to poor outcome in prostate cancer patients. Prostate 2009;69:799–809.

26. Hägglöf C, Hammarsten P, Josefsson A, Stattin P, Paulsson J, Bergh A, Östman A. Stromal PDGFRß expression in prostate tumors and non-malignant prostate tissue predicts prostate cancer survival. PLoS ONE 2010;5:e10747.

27. Hammarsten P, Karalija A, Josefsson A, Rudolfsson SH, Wikström P, Egevad L, Granfors T, Stattin P, Bergh A. Low levels of phosphorylated epidermal growth factor receptor in nonmalignant and malignant prostate tissue predict favorable outcome in prostate cancer patients. Clin Cancer Res 2010;16:1245–1255.

28. Johansson A, Rudolfsson S, Hammarsten P, Halin S, Pietras K, Jones J, Stattin P, Egevad L, Granfors T, Wikström P, Bergh A. Mast cells are novel independent prognostic markers in prostate cancer and represent a target for therapy. Am J Pathol 2010;177:1031–1041.

29. Josefsson A, Adamo H, Hammarsten P, Granfors T, Stattin P, Egevad L, Laurent AE, Wikström P, Bergh A. Prostate cancer increases hyaluronan in surrounding nonmalignant stroma, and this response is associated with tumor growth and an unfavorable outcome. Am J Pathol 2011;179:1961–1968.

30. Thomasson M, Wang B, Hammarsten P, Dahlman A, Persson JL, Josefsson A, Stattin P, Granfors T, Egevad L, Henriksson R, Bergh A, Hedman H. LRIG1 and the liar paradox in prostate cancer: A study of the expression and clinical significance of LRIG1 in prostate cancer. Int J Cancer 2011;128:2843–2852.

31. Josefsson A, Wikström P, Egevad L, Granfors T, Karlberg L, Stattin P, Bergh A. Low endoglin vascular density and Ki67 index in Gleason score 6 tumours may identify prostate cancer patients suitable for surveillance. Scand J Urol Nephrol 2012;46:247–257.

32. Fowler CJ, Hammarsten P, Bergh A. Tumour cannabinoid CB_1 receptor and phosphorylated epidermal growth factor receptor expression are additive prognostic markers for prostate cancer. PLoS ONE 2010;5:e15205.

33. Chung SC, Hammarsten P, Josefsson A, Stattin P, Granfors T, Egevad L, Mancini G, Lutz B, Bergh A, Fowler CJ. A high cannabinoid CB_1 receptor immunoreactivity is associated with disease severity and outcome in prostate cancer. Eur J Cancer 2009;45:174–182.

34. Cudaback E, Marrs W, Moeller T, Stella N. The expression level of CB_1 and CB_2 receptors determines their efficacy at inducing apoptosis in astrocytomas. PLoS ONE 2010;5:e8702.

35. R Core Team: R. A language and environment for statistical computing. R Foundation for Statistical Computing, Vienna, Austria. ISBN 3-900051-07-0. http://www.R-project.org/. 2012.

36. Shao Y-H, Demissie K, Shih W, Mehta AR, Stein MN, Roberts CB, Dipaola RS, Lu-Yao GL. Contemporary risk profile of prostate cancer in the United States. J Natl Cancer Inst 2009;101:1280–1283.

37. Tsamardinos I, Brown LE, Aliferis CF. The max-min hill-climbing Bayesian network structure learning algorithm. Mach Learn 2006;54:31–78.

38. Minner S, Jessen B, Stiedenroth L, Burandt E, Köllermann J, Mirlacher M, Erbersdobler A, Eichelberg C, Fisch M, Brümmendorf TH, Bokemeyer C, Simon R, Steuber T, Graefen M, Huland H, Sauter G, Schlomm T. Low level HER2 overexpression is associated with rapid tumor cell proliferation and poor prognosis in prostate cancer. Clin Cancer Res 2010;16:1553–1560.

39. Isaacs J, Isaacs W, Feitz F, Scheres J. Establishment and characterization of seven Dunning rat prostatic cancer cell lines and their use in developing methods for predicting metastatic abilities of prostatic cancers. Prostate 1986;9:261–281.

40. Halin S, Rudolfsson SH, Van Rooijen N, Bergh A. Extratumoral macrophages promote tumor and vascular growth in an orthotopic rat prostate tumor model. Neoplasia 2009;11:177–186.

41. McCullough DJ, Nguyen LM, Siemann DW, Behnke BJ. Effects of exercise training on tumor hypoxia and vascular function in the rodent preclinical orthotopic prostate cancer model. J Appl Physiol 2013;115:1846–1854.

42. Thors L, Eriksson J, Fowler CJ. Inhibition of the cellular uptake of anandamide by genistein and its analogue daidzein in cells with different levels of fatty acid amide hydrolase-driven uptake. Br J Pharmacol 2007;152:744–750.

43. Fowler CJ, Ghafouri N. Does the hydrolysis of 2-arachidonoylglycerol regulate its cellular uptake? Pharmacol Res 2008;58:72–76.

44. Conticello C, Pedini F, Zeuner A, Patti M, Zerilli M, Stassi G, Messina A, Peschle C, De Maria R. IL-4 protects tumor cells from anti-CD95 and chemotherapeutic agents via up-regulation of antiapoptotic proteins. J Immunol 2004;172:5467–5477.

45. Börner C, Bedini A, Höllt V, Kraus J. Analysis of promoter regions regulating basal and interleukin-4-inducible expression of the human CB1 receptor gene in T lymphocytes. Mol Pharmacol 2008;73:1013–1019.

46. Maccarrone M, Valensise H, Bari M, Lazzarin N, Romanini C, Finazzi-Agrò A. Progesterone up-regulates anandamide hydrolase in human lymphocytes: Role of cytokines and implications for fertility. J Immunol 2001;166:7183–7189.

47. Hart S, Fischer O, Ullrich A. Cannabinoids induce cancer cell proliferation via tumor necrosis factor α-converting enzyme (TACE/ADAM17)-mediated transactivation of the epidermal growth factor. Cancer Res 2004;64:1943–1950.

48. Grimsey N, Goodfellow C, Scotter E, Dowie M, Glass M, Graham E. Specific detection of CB_1 receptors; cannabinoid CB_1 receptor antibodies are not all created equal. J Neurosci Meth 2008;171:78–86.

49. Du H, Kwon I-K, Kim J. Neuregulin-1 impairs the long-term depression of hippocampal inhibitory synapses by facilitating the degradation of endocannabinoid 2-AG. J Neurosci 2013;33: 15022–15031.

50. Rozenfeld R, Devi LA. Regulation of CB_1 cannabinoid receptor trafficking by the adaptor protein AP-3. FASEB J 2008;22:2311–2322.

51. Lurje G, Lenz H-J. EGFR signaling and drug discovery. Oncology 2009;77:400–410.

52. De Miguel P, Royuela Bethencourt R, Ruiz A, Fraile B, Paniagua R. Immunohistochemical comparative analysis of transforming growth factor α, epidermal growth factor, and epidermal growth factor receptor in normal, hyperplastic and neoplastic human prostates. Cytokine 1999;11:722–727.

53. Neto AS, Tobias-Machado M, Wroclawski ML, Fonseca FLA, Teixeira GK, Amarante RDM, Wroclawski ER, Del Giglio A. Her-2/*neu* expression in prostate adenocarcinoma: A systematic review and meta-analysis. J Urol 2010;184:842–850.

54. Michalski C, Oti F, Erkan M, Sauliunaite D, Bergmann F, Pacher P, Batkai S, Müller M, Giese N, Friess H, Kleeff J. Cannabinoids in pancreatic cancer: Correlation with survival and pain. Int J Cancer 2008;122:742–750.

55. Gustafsson SB, Palmqvist R, Henriksson ML, Dahlin AM, Edin S, Jacobsson SOP, Oberg Å, Fowler CJ. High tumour cannabinoid CB_1 receptor immunoreactivity negatively impacts disease-specific survival in stage II microsatellite stable colorectal cancer. PLoS ONE 2011;6:e23003.

56. Xu X, Liu Y, Huang S, Liu G, Xie C, Zhou J, Fan W, Li Q, Wang Q, Zhong D, Miao X. Overexpression of cannabinoid receptors CB1 and CB2 correlates with improved prognosis of patients with hepatocellular carcinoma. Cancer Gen Cytogen 2006;171: 31–38.

57. Messalli EM, Grauso F, Luise R, Angelini A, Rossiello R. Cannabinoid receptor type 1 immunoreactivity and disease severity in human epithelial ovarian tumors. Am J Obstet Gynecol 2014; in press doi: 10.1016/j.ajog.2014.04.004